APPLICATION OF ADAPTIVE PYRAMIDAL DUAL-TREE DIRECTIONAL FILTER BANK IN GROUND ROLL ATTENUATION

SEYED AHMAD MORTAZAVI[1], ABDOLRAHIM JAVAHERIAN[1,2], MAJID NABI BIDHENDI[2], HAMID REZA AMINDAVAR[3], SIYAVASH TORABI[4] and MOHAMMAD REZA BAKHTIARI[5]

[1] *Department of Petroleum Engineering, Amirkabir University of Technology, Tehran, Iran.*
[2] *Institute of Geophysics, University of Tehran, Tehran, Iran. javaheri@ut.ac.ir*
[3] *Department of Electrical Engineering, Amirkabir University of Technology, Tehran, Iran.*
[4] *Dana Geophysics Company, Tehran, Iran.*
[5] *National Iranian Oil Company, Exploration Directorate, Tehran, Iran.*

(Received January 2, 2016; revised version accepted November 21, 2016)

ABSTRACT

Mortazavi, S.A., Javaherian, A., Bidhendi, M.N., Amindavar, H.R., Torabi, S. and Bakhtiari, M.R., 2017. Application of adaptive pyramidal dual-tree directional filter bank in ground roll attenuation. *Journal of Seismic Exploration*, 26: 49-79.

Ground roll is a coherent noise that may mask reflections in a fan-shaped zone. Its attenuation, accordingly, is of utmost significance in seismic data processing. Different methods have been developed to attenuate ground roll. In this paper, an adaptive pyramidal dual-tree directional filter bank (PDTDFB) was applied to a synthetic data consisting of ground roll, aliased ground roll, and reflections over an earth model and implemented on two shot records from the west and south of Iran. PDTDFB is a multiscale and a multidirectional filter with a dual-tree structure which decomposes an image (or a shot record) to various directional subscales in different scales. Certain subscales predominantly contain ground roll, and aliased ground roll, having higher values of energy than others. In the first step, through adaptively detecting these subscales via energy calculation, ground roll and aliased ground roll are attenuated. In the second step, the remaining aliased ground roll is adaptively attenuated. According to the results of synthetic and real data, the adaptive PDTDFB highly attenuated the ground roll and aliased ground roll with minimum harm to signals. We further examined the effects of random noise and residual statics when using the adaptive PDTDFB in ground roll attenuation. The adaptive PDTDFB is not too sensitive to the level of random noise. Moreover, the performance of the filter is acceptable in the presence of residual statics. Also, according to the comparison with f-k and SVD filters and the qualitative and quantitative assessments, the proposed filter entailed better results than f-k and SVD filter, especially as far as aliased ground roll attenuation is concerned.

KEY WORDS: aliased ground roll attenuation, signal-to-noise-ratio, directional filter bank, adaptive pyramidal dual-tree directional filter bank.

0963-0651/17/$5.00

INTRODUCTION

There are many types of coherent and incoherent noises in seismic reflection data such as ground roll, multiples, near-surface scattered energy, airwaves, random noise, and guided waves. These noises can affect the quality of seismic data and have to be attenuated in seismic data processing. Ground roll is a particular type of Rayleigh wave which, compared to signals, has high amplitudes, low frequencies, and low velocities. Such Rayleigh wave is dispersive, i.e., in general, the higher the frequency the lower its velocity will be. In a fan-shaped zone, ground roll masks reflections, particularly shallow reflections in the near offset and deep reflections in the far offset. Aliased ground roll, having a slope similar to signals, is another challenge in ground roll attenuation.

There exist many methods for ground roll attenuation, the most conventional being f-k filtering which attenuates ground roll with regard to the differences in velocity and frequency between the ground roll and signals (Yilmaz, 2001, P. 898). However, f-k filter may not be able to remove the aliased ground roll when it has an overlap with the reflections in the f-k domain. The tau-p method, another conventional method for ground roll attenuation (Yilmaz, 2001, P 920), is based on the difference between the ground roll and the reflections in as far as wave parameter values are concerned. The forward and the inverse transforms of this method do not show a unique response, causing some unreal events and artifacts. K-L and singular value decomposition (SVD) are yet another ground roll suppression methods based on the eigenimages decomposition. Liu (1999) proposed a method that could flatten the ground roll and suppress it using the first eigenvalues via K-L transform. Tyapkin et al. (2003) employed the data alignment method of Liu (1999) to make the coherent noise horizontally aligned with one or more time horizons of a common shot gather. Lu (2006) presented an adaptive SVD filter to enhance non-horizontal events by detecting seismic image texture and to improve the horizontal alignment of the estimated dip through data rotation. Bekara and Baan (2007) proposed a local SVD approach to noise removal. Porsani et al. (2010) proposed an SVD filtering method for ground roll attenuation where prior to SVD computation, the normal move-out (NMO) correction is applied to the data, with the purpose of flattening and constructing the reflections, and, later, applying an inverse NMO. Mortazavi and Javaherian (2013) designed an adaptive method using SVD transform and discussed the effect of random noise in ground roll attenuation. Boustani et al. (2013) combined curvelet transform and SVD to enhance the performance of each method. Radial transform, used by Henley (1999, 2003), is another method for ground roll attenuation, where the data is transformed from the time-offset domain to the time-apparent velocity domain. By using a band-pass filter and applying an inverse radial transform, the ground roll can ultimately be attenuated. Chang et al. (2011) proposed a

method that fitted the best polynomial curve to the ground roll in the radial domain and reconstructed it in the time domain. Manentti and Porsani (2013) combined radial and SVD for ground roll attenuation. Curvelet, wavelet, and shearlet transforms are other methods that can be employed in attenuating ground roll. Owing to the differences between ground roll and the signals in velocity and frequency content, the preceding methods can separate noise and signals in different subscales. In this regard, Yarham et al. (2006) and Zhang et al. (2010) used the curvelet transform; Hamidi et al. (2013) employed the wavelet transform, and Hosseini et al. (2015) used the shearlet transform in ground roll suppression.

Directional filter bank (DFB), pyramidal directional filter bank (PDFB) and pyramidal dual-tree directional filter bank (PDTDFB), as the major methods incorporated in the present paper, have not been extensively used in the seismic data processing (ground roll attenuation, for instance). Such methods, nonetheless, are very common in image processing. For example, Khan et al. (2004) used DFB method as a part of the enhancement of an angiogram image for separating various directional vessels. Alecu et al. (2007) used PDFB to propose a generic hybrid oriented-transform and wavelet-based image representation for intra-band image coding. Ma et al. (2010) proposed an edge detection method using PDFB. Niu et al. (2011) introduced a new color image watermarking algorithm against geometric distortion based on the support vector regression and pyramidal dual-tree directional filter bank.

In the present research, we considered the concept of DFB and its derivatives and proposed an adaptive PDTDFB method for attenuating ground roll and aliased ground roll. The suggested method was tested over a synthetic shot record with aliased ground roll containing various signal-to-noise ratios (SNRs). The algorithm was then applied to two real data sets from the west and south of Iran. Also, the performance of the filter was compared with the f-k filtering and SVD filtering as conventional methods.

METHODOLGY

Theory and literature review

Bamberger and Smith (1992) introduced directional filter banks for image processing. DFB is a multi-directional method that can decompose an image to various directions. It does not, however, work properly over the low-frequency components of an image, and does not generate a sparse representation. To overcome these problems, DFB should be combined with other methods such as Laplacian pyramid (LP) introduced by Burt and Adelson (1983). LP is an image compression method that, as a multi-scale and multi-resolution technique, can represent various scales of an image. Combining Laplacian pyramid (as an

image multi-resolution or multiscale method which can demonstrate different scales of an image) and directional filter bank (as an image multi-directional method which can decompose directional components of an image). Do and Vetterli (2001, 2005) presented PDFB method. In this method, different scales of an image are primarily obtained by LP, and then DFB specifies the directional components of each subscale. Therefore, this technique can eliminate the drawbacks of DFB through directionally decomposing low-frequency components of an image. The main downside of PDFB is spatial aliasing effect during the reconstruction of the decomposed subscales. As a solution, Nguyen (2006) proposed a newer version of the PDFB method called pyramidal dual-tree-directional filter bank (PDTDFB) which employs a dual-tree algorithm that minimizes the spatial aliasing of image components and causes lower artifacts. These methods are not usually used in seismic data processing; rather they are conventional methods related to image processing. The four sections below provide the mathematics of each method with further explanation.

Directional Filter Bank

DFB is a multidirectional method that can decompose an image into different directional components. Fig. 1a shows a frequency partitioning of the DFB in the case of 8 channels, using an n-level iterated tree-structured filter bank. This method generates 2D directional information (Do and Vetterli, 2001), and employs the Quincunx Filter Bank (QFB) together with modulations and rotations in its algorithm to decompose an image into various directions. A re-sampling is also needed in the algorithm. By using resampling matrices (R), rotations in DFB can be obtained. The determinant of R matrices is ± 1, and they represent a rearrangement of the input samples.

After certain modifications, the impulse response of the filter is (Do and Vetterli, 2001):

$$g[n] = \int_0^{\pi} dw_2 \int_{lw_2/N}^{(l+1)w_2/N} dw_1 (e^{jw^T n} + e^{-jw^T n})$$

$$= (2\pi/n_1)[\psi\{n_1(l+1)/N + n_2\} - \psi\{n_1 l/N + n_2\}] \quad , \qquad (1)$$

where $N = 2^{n-2}$, $w_1 = lw_2/N$, $w_1 = (l + 1)w_2/N$, $l = -N, \ldots, N-1$, and $\psi(x) = [1 - \cos(\pi x)]/\pi x$. According to eq. (1), g[n] is the subtraction of two ridge functions damped by $1/n_1$ and oriented around the line $n_2 = -n_1 l/N$ (Do and Vetterli, 2001).

Laplacian pyramid

Laplacian pyramid is a multi-scaling or multi-resolution method for image compression. This method is not used for ground roll attenuation in seismic data processing. However, as said above, PDFB (combination of LP and DFB) can be used for ground roll attenuation. In LP method, a net data compression is achieved by subtracting low-pass filtered image from the original image, and eliminating the pixel-to-pixel correlations. Quantizing the difference image provides further data compression. Repeating these steps and the low-pass filtered version of the image is compressed. Iteration of the process at appropriately expanded scales generates a pyramid data structure. In brief, such procedure produces the various scales of an image (Burt and Adelson, 1983). The first (bottom) level of the LP is constructed by encoding the error image which remains when an expanded reduced image G_1 that is a prediction for pixel values in the original image is subtracted from the original image G_0, rendering a compressed representation. By encoding G_1 through the same procedure, the next LP level can be achieved (Burt and Adelson, 1983). LP is a set of error images between two levels of the Gaussian pyramid L_0, L_1, ..., L_N. Accordingly, for $0 < k < N$ (Burt and Adelson, 1983), in eq. (2), G is an image employed for image compression,

$$L_k = G_k - \text{EXPAND}\,(G_{k+1}) \ , \qquad (2)$$

where there is no image G_{N+1} to be the prediction image for G_N, hence the assumption that $L_N = G_N$ (Burt and Adelson, 1983). One drawback of DFB is that it does not give a sparse representation owing to the leakage of low-frequency components of the image into several directional subscales, the reason for which is that DFB takes the high frequencies, hence the fact that the low-frequency components of an image are handled poorly (Fig. 1a). Accordingly, if the low-frequency components are subtracted prior to applying the DFB, better results can be achieved (Do and Vetterli, 2001).One way to overcome low-frequency components problem is to use the LP introduced by Burt and Adelson (1983) where the LP decomposition at each step results in sampled low-pass image. In order to have a band-pass version of the image, the original image is subtracted from the generated image (Do and Vetterli, 2001).

Pyramidal Directional Filter Bank

As said earlier, DFB cannot work properly over the low-frequency components of an image, and it cannot provide a sparse representation. In order to overcome the sparsity problem in DFB, Do and Vetterli (2001) combined DFB with a multiresolution pyramid where maximum information is packed into a small number of samples. The new approach (PDFB) is a multi-directional multiscale method created through the combination of LP and DFB. Applying

DFB on band-pass images, and directional information can be well obtained. Fig. 1b shows the pyramidal directional filter bank where if the plan on the coarse image is iterated repeatedly, better results can be gained. The PDFB is perfectly reconstructed (PR), hence a frame operator for 2D signals. The redundancy of PDFB is up to 33%, the same as LP when sub-sampled by two in each dimension. Image decomposition is provided by the following equation (Do and Vetterli, 2001),

$$\|x\|^2 = \sum_{j=1}^{J} \|b_j\|^2 + \|a_j\|^2 \quad , \tag{3}$$

where x is the input image decomposed into a low-pass image a_j and J band-pass image b_j, j = 1, 2, ..., J. The DFB also decomposes each band-pass image b_j into the directional coefficients d_j with $\|b_j\|^2 = \|d_j\|^2$. By substituting b_j by d_j we have: $x \rightarrow (d_1, d_2, \ldots, d_j, a_j)$. Decomposition by DFB can also conserve energy (Do and Vetterli, 2001),

$$\|x\|^2 = \sum_{j=1}^{J} \|d_j\|^2 + \|a_j\|^2 \quad . \tag{4}$$

Pyramidal Dual-Tree Directional Filter Bank

Proposed by Nguyen (2006) to attenuate the effect of the spatial aliasing, PDTDFB is a dual-tree algorithm of the PDFB method. The PDTDFB approach decomposes an image into variant subscales, each component of the original image. If each subscale in DFB domain is reconstructed and returned to the initial domain, the original image can be achieved by superimposing all reconstructed subscales. A shift-invariant PDTDFB is generated by combining a shift-invariant LP with the dual-tree DFB. Also, a combination of a multiresolution FB (filter bank) with a dual-tree DFB at high frequency is used to create a shiftable multiscale and multidirectional decomposition. Such combination provides a multiresolution image decomposition that can eliminate the remaining aliasing effect in the PDTDFB. The potential cause of aliasing in the dual-tree structure is the high-frequency components near $(\pm\pi,0)$ and $(0,\pm\pi)$. As is shown in Fig. 1c, to attenuate the effect of aliasing, an undecimated two-channel FB [low-pass filter $L_0(z)$ and high-pass filter $R_0(z)$] is implemented to filter the frequency components (Nguyen, 2006). For the undecimated FB to be PR (perfectly reconstructed), these low-pass and high-pass filters have to be in accord with the following equation (Nguyen, 2006)

$$|L_0(w)|^2 + |R_0(w)|^2 = 1 \quad . \tag{5}$$

At the first level, the pyramidal FB, the output of $L_0(z)$, is divided into two parts: the coarse approximation and the high-frequency component (points L and H in Fig. 1c, respectively). A dual-tree of the DFBs is then applied to this high-frequency component to have higher order decomposition and generate the real and imaginary parts of the directional subscales of the 2^n complex (block P). By repeating this part at the low-frequency output (point L), a pyramid is produced. The filters in blocks P and Q satisfy the PR and non-aliasing conditions (Nguyen, 2006)

$$|R_1(w)|^2 + \tfrac{1}{4}|L_1(w)|^2 = 1, \text{ and } L_1(w_1,w_2) = 0 \ . \tag{6}$$

If $\min(|w_1|, w_2|) > \pi/2$, Fig. 1c can demonstrate the first level of the PDTDFB, where P and Q can be repeated to provide a multiscale decomposition. The image representation generated according to the arrangement in Fig. 1c is shiftable. Moreover, the DFBs used in the PDTDFB are constructed employing the proposed structure of Bamberger and Smith (1992). Except for the second level, the primal and dual DFBs in the dual-tree structure are identical at each level (Nguyen, 2006).

The directional filters of the analyzed primal and dual DFBs are $H_i(z)$ and $H_i^H(z)$, $i \in \{0, 1, \ldots, 2^n-1\}$; $\tilde{H}_i(z)$and $\tilde{H}_i^H(z)$ are the equivalent primal and dual analysis filters of the first level of PDTDFB, transforming input x(n) to outputs $H_i(z)$ and $H_i^H(z)$. In the same way, $F_i(z)$ and $F_i^H(z)$ are the equivalent synthesis filters; $\tilde{F}_i(z)$ and $\tilde{F}_i^H(z)$ are those on the synthesis side (Fig. 1c) whose frequency responses are as follows (Nguyen, 2006)

$$\tilde{H}_i(w) = L_0(w)R_1(w)H_i(w) \ , \tag{7}$$

$$\tilde{H}_i^H(z) = L_0(w)R_1(w)H_i^H(w) \ , \tag{8}$$

$$\tilde{F}_i(w) = L_0(-w)R_1(-w)F_i(w) \ , \tag{9}$$

$$\tilde{F}_i^H(z) = L_0(-w)R_1(-w)F_i^H(w) \ . \tag{10}$$

The redundant ratios of PDFB and PDTDFB are 4/3 and 11/3, respectively (Nguyen, 2006). Therefore, PDTDFB has a lower redundant ratio in comparison to PDFB. The conventional DFB is constructed by a binary tree of two-channel FBs that are obtained from one prototype fan FB if appropriate resampling blocks are employed in the tree. By cascading two-channel FBs, using the same prototype fan FBs [$H_0^{(f)}(z)$ and $H_1^{(f)}(z)$] and resampling the blocks, the 2-channel dual-tree DFB is constructed from the mentioned four-channel dual-tree DFB. Accordingly, each directional filter pair in the primal and dual 2^n-channel DFBs still forms a Hilbert transforms pair. Considering the two branches together, the aliasing elements partially cancel out each other as in

four-channel dual-tree DFB (Nguyen, 2006). Nguyen (2006) proposed a dual-tree algorithm for the PDFB method to reduce the effect of spatial aliasing, a new method named PDTDFB. PDFB and PDTDFB methods can decompose an image into many different subscales each with a component of the original image. If every subscale in DFB domain is reconstructed and returned to the original domain, the original image can be achieved by superimposing all the reconstructed subscales.

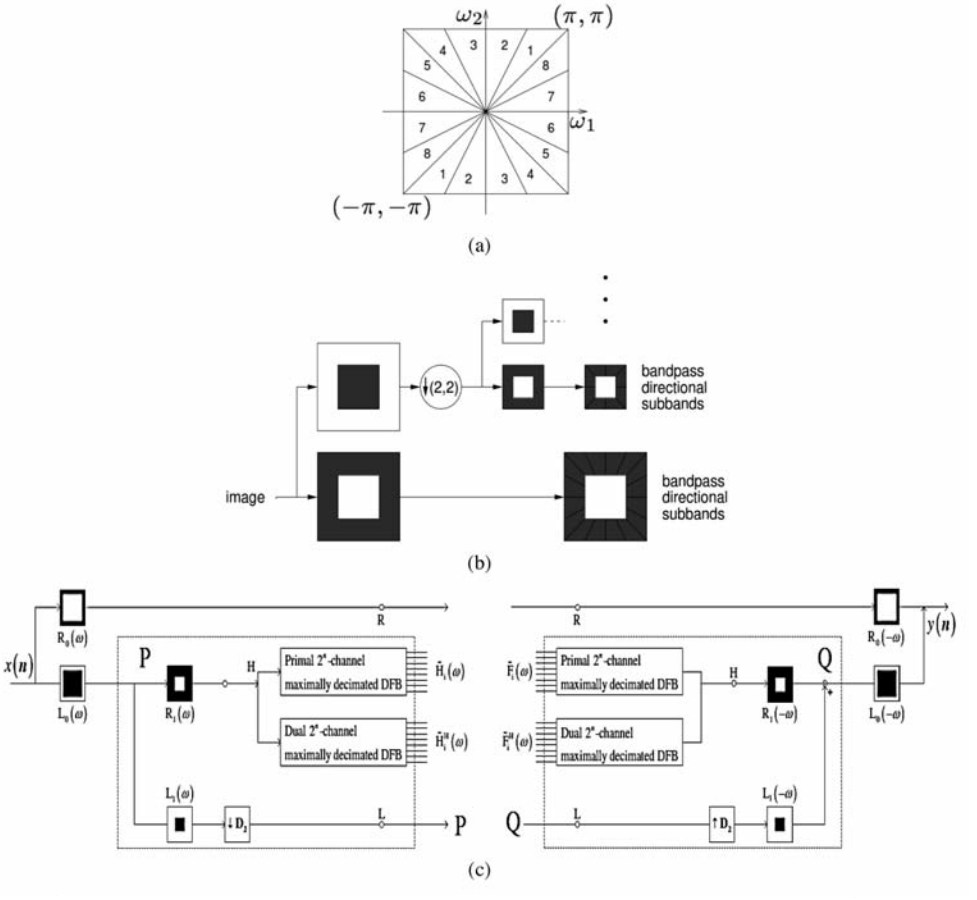

Fig. 1. (a) Directional filter bank frequency partitioning (Do and Vetterli 2001). (b) A multiscale decomposition into octave bands is computed by the Laplacian pyramid; then a directional filter bank is applied to each band-pass channel (Do and Vetterli, 2005). (c) The structure of the PDTDFB: decomposition and reconstruction. Similar P and Q blocks can be reiterated at lower scales to decompose an image into a multiscale representation (Nguyen, 2006).

As shown in Fig. 1b, the PDFB method has two main parameters: (1) the number of the levels (scales) of the transform and (2) the number of the directional subscales in each level. It is notable that the central subscale (or center subscale) in Fig. 1b is not directionally decomposed. On the other hand, through the selection of a lower number of levels, most data energy will be concentrated on the center subscale, hence the more the levels, the better the energy will be distributed. The size of the subscale matrices in the PDTDFB domain is related to the number of directional subscales in each level, decreasing with the increase in the number of directional subscales. The matrices with tiny dimensions are not suitable for investigation hence the fact that the number of levels and subscales must be optimized, a matter further discussed in the "effective parameters" section.

A seismic shot record consists of different events such as ground roll, random noise, reflections, and refractions, each with their own unique characteristics, appearing in various subscales in the PDTDFB domain. Fig. 2a illustrates a synthetic shot record of an earth model with seven layers as in Table 1.

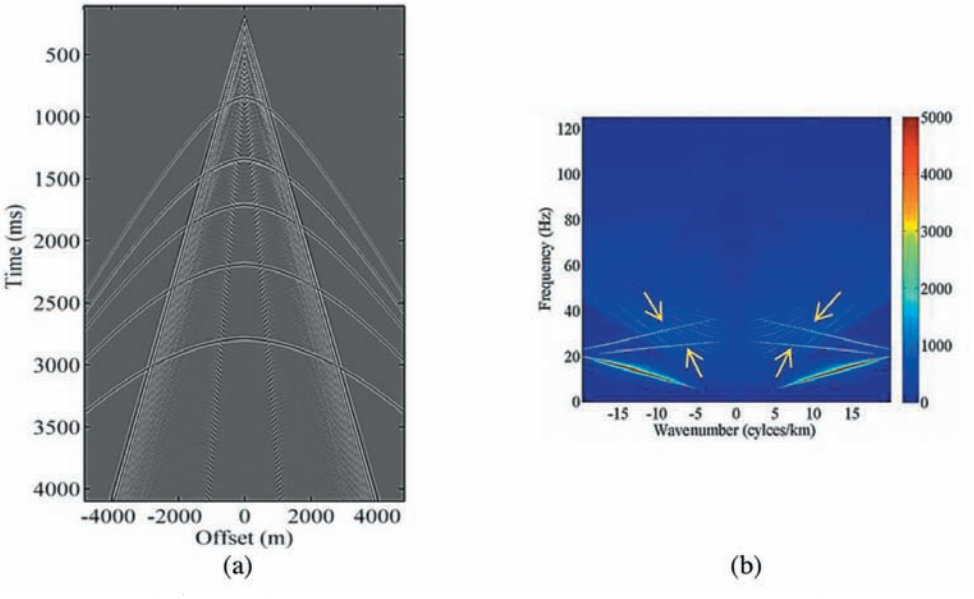

Fig. 2.(a) A synthetic shot record of an earth model with 7 layers in which the 1st two layers are weathered (Table 1) with a sampling interval of 4 ms, trace spacing of 25 m, near offset of 200 m, and 14 m source depth. The arrows represent the aliased ground roll. Using the frequency-wavenumber method, we produced the ground roll by Seismology software (Herrmann, 2013). Reflections were generated by MATLAB. (b) The f-k spectrum of (a).

In this figure, the sampling interval, trace spacing, and the near offset are 4 ms, 25 m, and 200 m, respectively, with the source located at a depth of 14m. Using the frequency-wave number method, the ground roll was produced by the Computer Program of Seismology software (Herrmann, 2013), and the reflections were generated by MATLAB. Fig. 2b shows the f-k spectrum of Fig. 2a. In Fig. 2b, arrows refer to the aliased ground roll which contaminates the signals, and whose attenuation is an ineluctable issue in seismic data processing. Fig. 3a is a sample subscale that predominantly contains reflections in the PDTDFB domain. Figs. 3b and 3c show subscales mainly consisting of ground

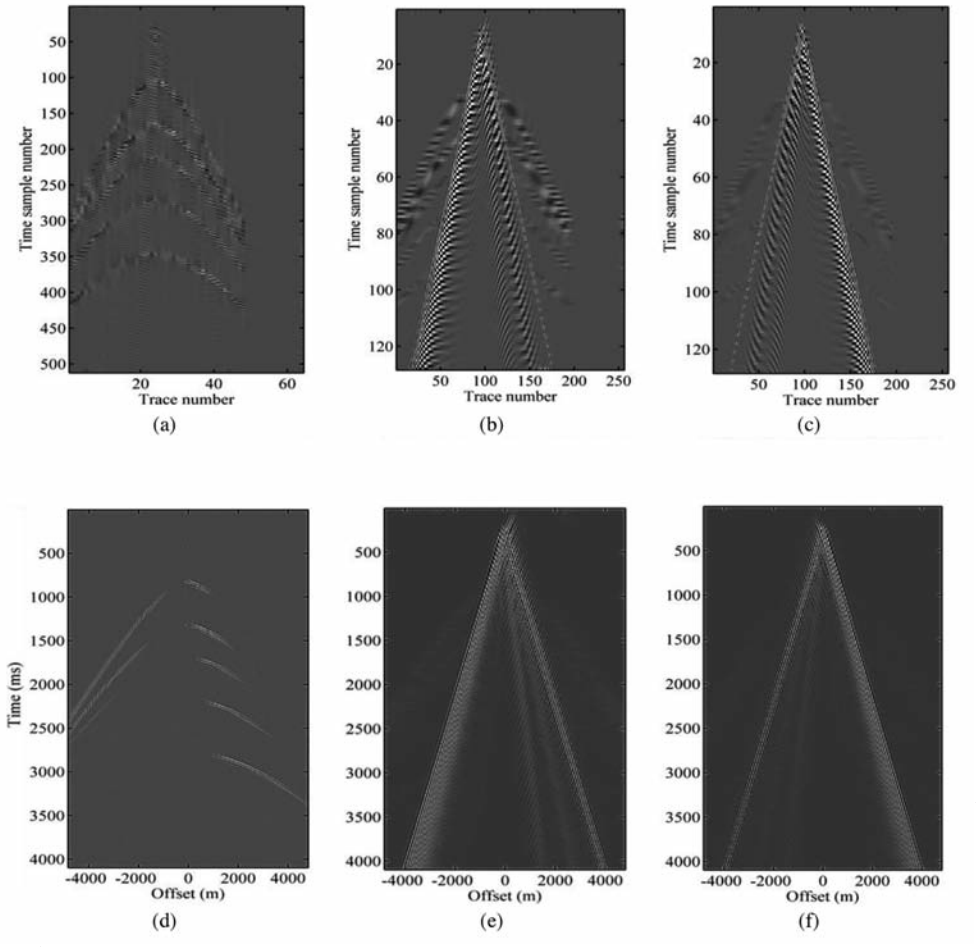

Fig. 3. Subscales in the PDTDFB domain consisting of: (a) reflections, (b) non-aliased and (c) aliased ground roll. (d-f) The time-domain presentations of (a-c).

roll and aliased ground, respectively. Each mentioned subscale was reconstructed to the time domain, Figs. 3d to 3f illustrating the reconstructed images of (a) to (c), respectively. It should be mentioned that the input PDTDFB is applied to the input matrices with dimensions of the power of two, zero columns or rows must be added to the input data, a process called zero padding. Following the application of the algorithm, the added columns or rows are deleted. The dimensions of the subscale matrices are different in each level. However, the dimensions do not change in the same subscales of each PDTDFB tree.

Table 1. Earth model for generating the synthetic shot record of Fig. 2a.

Layer no.	Thickness (km)	P-wave velocity (km/s)	S-wave velocity (km/s)	Density (gr/cc)
1	0.003	0.7	0.25	1.4
2	0.01	1.9	1.1	1.8
3	0.9	2.2	1.2	2
4	0.6	2.4	1.4	2.2
5	0.5	2.7	1.5	2.4
6	0.7	2.9	1.6	2.5
7	0.9	3	1.7	2.7
	Half space	3.3	1.9	2.8

Adaptive PDTDFB for ground roll and aliased ground roll attenuation

The PDTDFB decomposes an image into different subscales with various scales and directions. The original image is obtained once all reconstructed subscales are superimposed. PDTDFB uses a dual-tree algorithm where in each tree; the input image is decomposed to certain levels (scales) and directions. Each level is almost similar to frequency partitioning and the subscales in each level are equal to the various directions. We designed an algorithm that adaptively distinguishes the subscales containing ground roll and aliased ground roll from other subscales mainly containing reflections or other events. The designed algorithm was applied via two steps:

Step one: Primarily, the optimum number of levels and directional subscales were chosen. These effective parameters are explained more in the effective parameter section. Next, PDTDFB was applied to the shot record (as an image). PDTDFB uses a dual-tree algorithm, where the character of events in a specific subscale is similar in both trees. Moreover, in each tree, and in a specific direction, the character of events is similar in the various levels (scales).

Considering these two notes, and in order to save time, an algorithm was designed to determine the subscales containing ground roll in the last level of the trees; similar subscales in other levels and trees were, then, considered as subscales containing ground roll. After applying forward PDTDFB, each subscale of the final level of the trees was transformed back to the time domain through performing inverse PDTDFB. Then a velocity filter (in a ground roll velocity range such as 500 to 1500 m/s) was applied to the subscales in the time domain; the fan shaped zone of the ground roll, therefore, remained unchanged. The energy of the remaining region was calculated for each subscale. The remained fan shaped region mainly contained ground roll and aliased ground roll, events having high amplitude and energy. Therefore, after sorting the subscales in a descending manner, considering the calculated energy, the subscales mostly containing ground roll or aliased ground roll stood in the first places of the energy graph, separated from subscales containing other events like reflections and/or random noise. Subscales with higher energy can, then, be selected by the user. Following these procedures, two options remain:

- *Option 1. Applying the filter to all parts of the input shot record*: The selected subscales are zeroed in all three levels in the PDTDFB domain. Therefore, the whole input shot record is filtered and the ground roll and aliased ground roll are attenuated dominantly.

- *Option 2. Applying the filter in the fan shaped ground roll region of the input shot record*: The mentioned velocity filter is applied to the input shot record, and forward PDTDFB is only applied to the fan shaped ground roll region. The selected subscales in all levels of both trees are zeroed in the PDTDFB domain. Therefore the ground roll and aliased ground roll are attenuated dominantly. After reconstructing, the outer part of the ground roll fan shaped region is added to the filtered data.

Step two: After step one, ground roll and aliased ground roll were mainly attenuated. To reach the complete attenuation of the aliased ground roll, the data should be adaptively re-filtered. All the remaining subscales were transformed to the time domain, and the following criteria were checked:

- If in the positive offsets in the subscale, the events with negative dips (e.g., aliased ground roll and back scatters) show higher values of energy in comparison to events with positive dips, the positive offset of those subscales are zeroed.

- If in the negative offsets in the subscale, the events with positive dips (e.g., aliased ground roll and back scatters) show higher values of energy compared to events with negative dips, the negative offset of those subscales are zeroed.

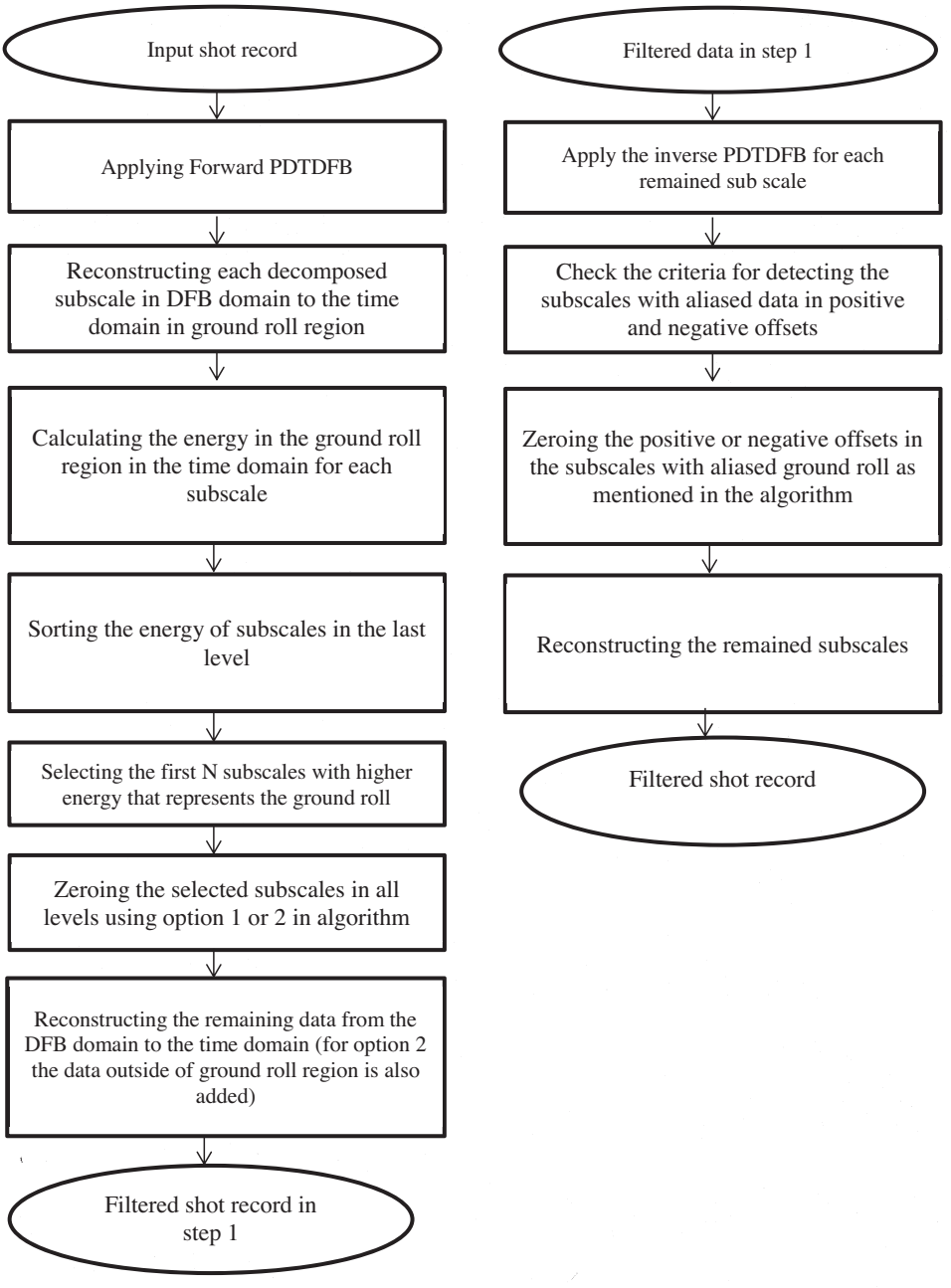

Fig. 4. Flowchart of the ground roll and aliased ground roll attenuation using the adaptive PDTDFB: (left) Step one and (right) Step two.

Fig. 4 shows the flowchart of the proposed adaptive PDTDFB method in two steps. Fig. 5a demonstrates the normalized energy of the subscales in the final level of the synthetic data in Fig. 6a. Fig. 5b is the sorted graph of part (a) according to the normalized energy in a descending manner. In Figs. 5a and 5b, 16 is the maximum value in the horizontal axis as it is the number of directions in the last level of the PDTDFB domain for the synthetic data, meaning that the last level, which is a scale from the original image, is divided into 16 directions. In Fig. 5a, the subscales with higher values of energy compared with others (for example 4 to 6 and 8) indicate ground roll or aliased ground roll. These events, in comparison with reflections and random noise, have higher energies in the mentioned fan shaped zone. On the other hand, the subscales of 1-3, and 9-16, in Fig. 5a indicate reflections or random noises because these have lower energies than the ground roll in the fan shaped zone. For instance, after sorting, subscales with an index number of 4 to 6 and 8 in 5a are equal to the first four subscales in Fig. 5b and indicate the ground roll. Therefore, in the first step of the algorithm, the first four subscales containing ground roll were selected for zeroing in both trees and all their levels.

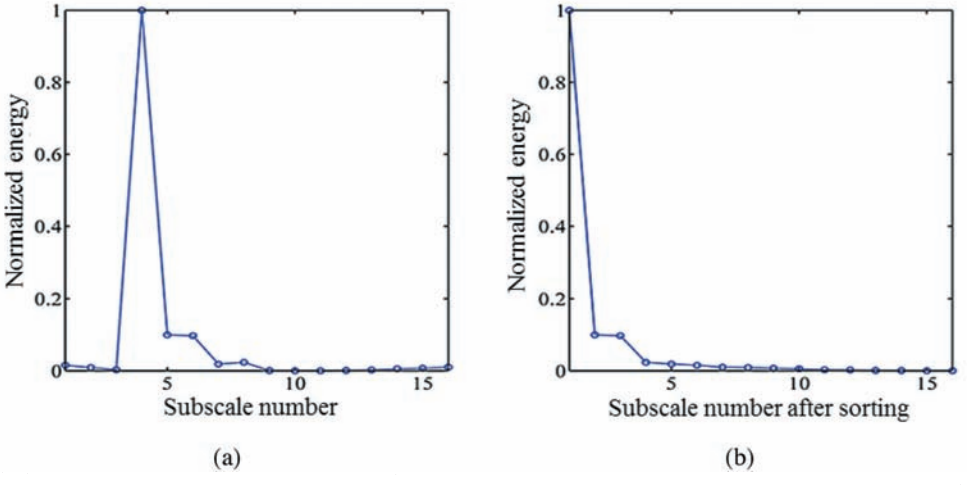

Fig. 5. (a) Normalized energy in the last PDTDFB level of each subscale in the time domain of Fig. 6a. (b) After sorting the normalized energy. Higher values of energy are allocated to subscales containing ground roll and aliased ground roll (for example subscales number 4-6 and 8 in part (a) are equal to the first 4 subscales after sorting which contain the ground roll).

Effective parameters

The following is mainly concerned with parameters effective on the performance of adaptive PDTDFB method:

1. **Number of levels and directional subscales**:

   These two parameters are the most effective parameters on the PDTDFB. Since this method has a dual-tree algorithm and is a multi-scale and multi-directional method, selecting the number of levels and directions in each level is important. Choosing a low number of levels results in the concentration of most energy and image content in the central level, not providing the possibility of separating different events like ground roll and reflections. On the contrary, choosing a high number of levels increases the calculation time while decreasing matrix dimensions in each subscale. Therefore, an optimum number of levels should be considered. There should also be an optimum number for directional subscales in each level to separate events with different dips. In a similar fashion, increasing the number of directional subscales augments the calculation time, while decreasing the number may lower the chances of separation.

2. **Range of selected velocity for determining ground roll region (fan shaped zone)**:

   According to methodology, in the last level of the trees, each subscale was reconstructed back to the time domain by applying inverse PDTDFB because the algorithm should decide which subscale mainly contains ground roll or aliased ground roll. After transforming each subscale to the time domain, a velocity filter was applied according to the velocity range of the ground roll. After that, the energy of the data in that filtered region was calculated, since the fan shaped region mainly contained ground roll or aliased ground roll and the aim was to recognize the subscales mainly containing ground roll. By choosing unsuitable low (as the minimum) ground roll velocity (e.g., 900 m/s) certain parts of the ground roll was placed out of the region and was not considered in the energy calculation; however, by selecting unsuitable higher values (e.g., 4000 m/s), certain reflections were placed in some subscales in the energy calculation region, hence the importance of determining the optimum velocity range (for example 500 to 1500 m/s).

3. **Number of subscales with high energy values**:

   As explained in the algorithm, after calculating the energy of each subscale in the ground roll region and the time domain, these subscales

were sorted based on their energy. Ground roll has higher amplitude (energy) than other events such as reflections and random noises, so subscales with high energy contain ground roll while others hold events such as reflections and/or random noises. The more the numbers of high-energy subscales, the higher the ground roll removal and the more the possibility of harm to reflections, and vice versa. As a result, it is pivotal to specify the optimum number of selected subscales with high values of energy.

4. **Option 1 or 2 in step one of the proposed algorithm**:

By using option 1, all parts of the shot record are used for applying the adaptive PDTDFB filter, in which case, the undesired events outside the ground roll fan shaped region are attenuated and cleaned up; option 1, however, takes more calculation time and may damage the signals outside of the ground roll region. Option 2, on the other hand, works faster and preserves more signals outside of the ground roll region, but the undesired events outside the ground roll remain in the data.

In each of the following synthetic or real examples, the values of the effective parameters are expressed.

EXAMPLES

Synthetic data

Fig. 6a shows the synthetic data set considering the earth model in Table 1. Fig. 6b is the filtered data of Fig. 6a obtained through the proposed adaptive PDTDFB, and (c) illustrates the difference between (a) and (b). In order to evaluate the performance of the filter, the f-k spectrum of each part is shown parallel to the seismic data. The arrows in (d) and (f) refer to the aliased ground roll. Fig. 6 illustrates that, while preserving the signals, the adaptive PDTDFB desirably attenuates the ground and aliased ground roll, whereas the f-k filtering damages the signals beneath the aliased ground roll. Fig. 7 shows the amplitude spectra of the input and filtered data, where the dash curve in the ellipse highlights the aliased ground roll, which, as shown, is considerably attenuated. Ground roll and aliased ground roll in this case are attenuated only in the ground roll fan shaped region (option 2 in step one of the algorithm). The optimum effective parameters for this data are as follows:

- number of levels: 3,
- number of directions: 16,
- range of velocity filter (m/s): 400-1100, and
- number of selected subscales with high energy: 4.

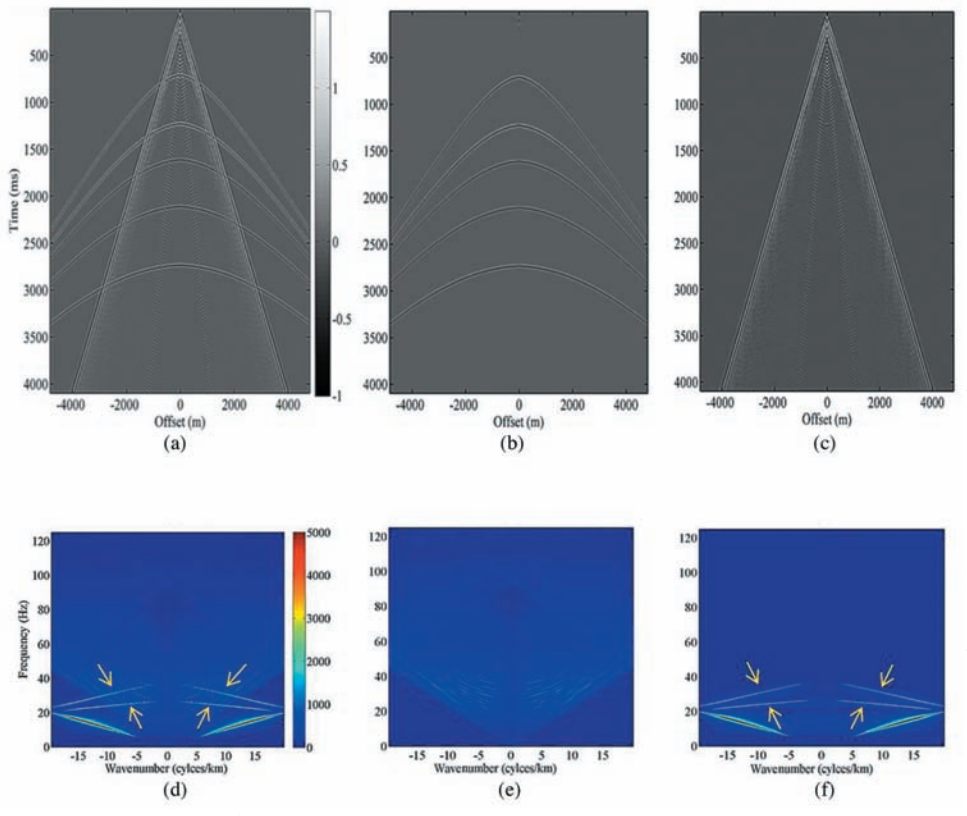

Fig. 6. (a) The synthetic shot record of an earth model of Table 1 with the sampling interval of 4 ms, near offset of 200 m, and receiver offset of 25 m. (b) Following the application of adaptive PDTDFB in ground roll attenuation. (c) The difference between (a) and (b). (d-f) F-k spectra of (a-c). The arrows represent the aliased ground roll.

Fig. 8 shows the performance of the adaptive PDTDFB filter in the presence of random noise and residual statics in order to test the de-noising experiment. Gaussian random noise was added to the synthetic data to reduce the signal-to-noise ratio (SNR); random statics of 0 to 12 ms was further added to the synthetic data to generate residual statics. It should be noted that, in the processing sequence, prior to ground roll attenuation, static corrections were applied, leaving only a residual statics in the data. In this section, the effect of residual statics is investigated on the performance of the filter in ground roll attenuation. Figs. 8(a-c) respectively demonstrate the synthetic data with SNR = 4, the data after applying adaptive PDTDFB filter, and the difference between (a) and (b). To investigate the performance of the filter, more random

noise was added to synthetic data; in order that the data set in part (d) has an SNR of 2. In the same way, (e) and (f) illustrate the filtered data and the difference between (d) and (e), respectively. Based on the results, the filter was not sensitive to the presence of random noise. Part (g) shows the synthetic data with added residual statics. Furthermore, parts (h) and (i) demonstrate the results following the application of the adaptive filter and the difference between (g) and (h), respectively. The generated residual statics were up to 12 ms. So as to better show the residual statics, a part of Figs. 8g to 8i with box was magnified at the bottom of each figure. The results indicate the success of the adaptive PDTDFB filter even in the presence of random noise and residual statics. Accordingly, ground roll and aliased ground roll were attenuated only in ground roll fan shaped region (option 2 in step one of the algorithm). The optimum parameters for the results in Fig. 8 are:

- number of levels: 3,
- number of directions: 16,
- range of velocity filter (m/s): 400-1100, and
- number of selected high-energy subscales: 4.

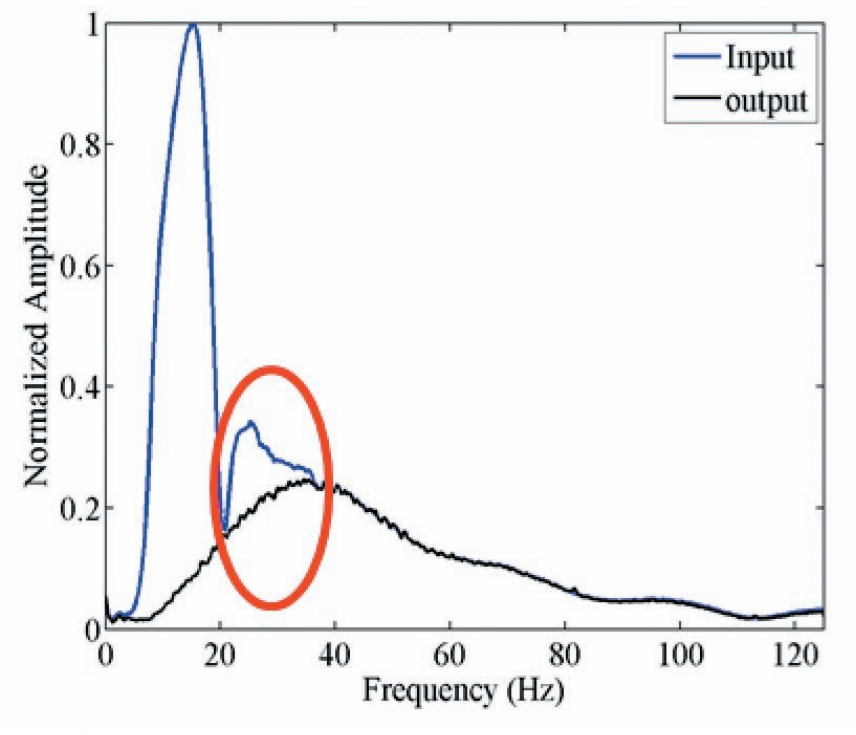

Fig. 7. Amplitude spectra of Figs. 6a and 6b. The dash curve in the ellipse shows the aliased ground roll.

Real data

The adaptive PDTDFB was applied to two real data sets from the west and south of Iran. Fig. 9a gives the normalized energy of the reconstructed subscales in the time domain of Fig. 10a. Part (b) is the descending order of the graph of (a) according to the energy of the subscales. The primary places in the graph with higher energy represent subscales predominantly containing ground roll and aliased ground roll. The filtered data of Fig. 10b was obtained through zeroing the aforementioned subscales in all levels while reconstructing the remaining subscales. Fig. 10a shows a shot record from the west of Iran with a sampling rate of 4 ms and trace spacing of 30 m. Parts (b) and (c) represent the data following the application of the adaptive PDTDFB and the difference between (a) and (b), respectively. In order to better evaluate the performance of the filter, the f-k spectrum of each part is shown parallel to the seismic data.

So as to investigate the performance of the filter in attenuating aliased ground roll in the presence of spatial aliasing, every other trace of Fig. 10a were omitted (Fig. 11a). After eliminating these traces, the trace interval became 60 m (Fig. 11a) from an initial 30 m (Fig. 10a), and as a result of such increase spatial aliasing was generated. The method was applied to the real data set after the production of aliased ground roll. Parts (b) and (c) respectively give the data after applying the filter and the difference between the input and output data. The f-k spectra of (a) to (c) are shown in (d) to (f), respectively. The arrows show the aliased ground roll considerably attenuated with minimum harm to the signals. Fig. 12 illustrates the amplitude spectrum of the input and the filtered data of Fig. 11. The assessments proved that the adaptive PDTDFB highly attenuated ground roll and aliased ground roll which were suppressed only in the ground roll fan shaped region (option 2 in step one of the algorithm). The optimum effective parameters for Figs. 10 and 11 are as follows:

- number of levels: 3,
- number of directions: 16,
- range of velocity filter (m/s): 500-1600, and
- number of the selected subscales with higher values of energy: 5.

To show the ability of the proposed method to filter and clean up other undesired events in the data, the adaptive PDTDFB was applied to another real data set from the south of Iran with a sampling interval of 2 ms, and trace spacing of 25 m. In this case, adaptive PDTDFB was applied to all parts of the shot record (option 1 in step one of the algorithm). Through the use of this option, the undesired events outside of the ground roll region and the refraction events were also cleaned up. Parts (a), (b) and (c) of Fig. 13a are respectively related to the input data, filtered data and the difference between the input and

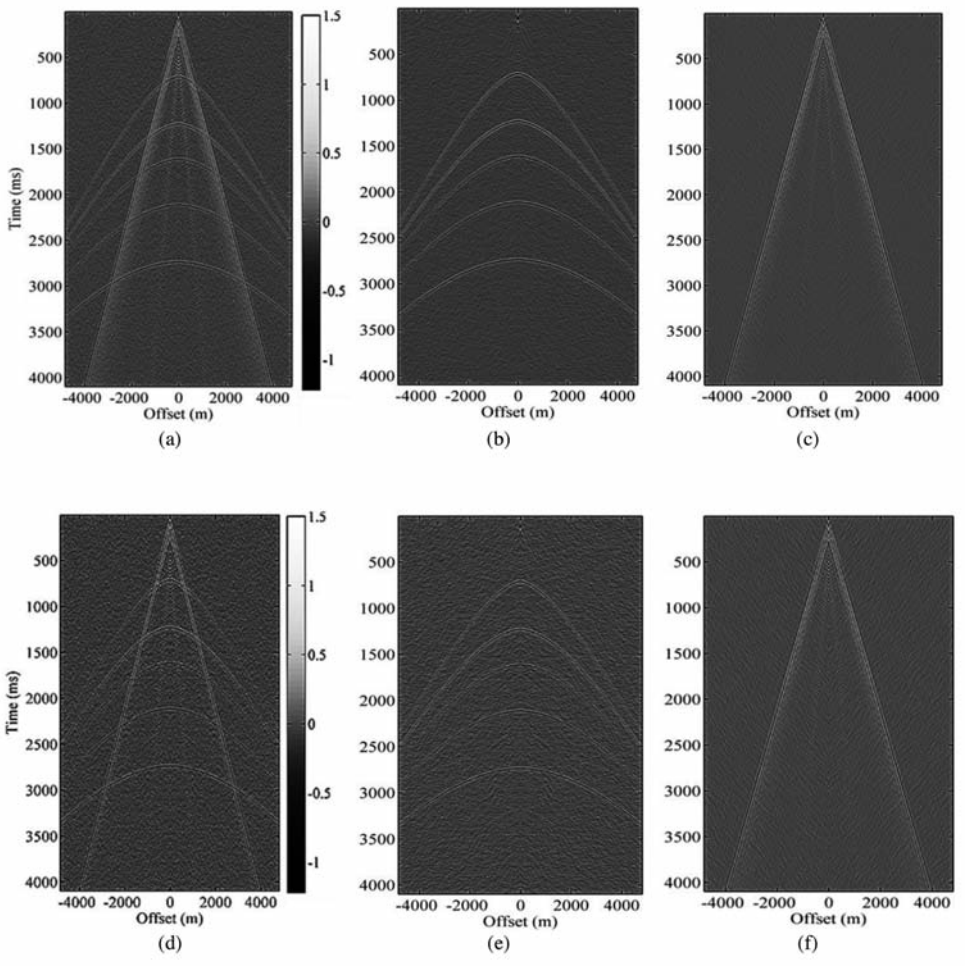

output data. Furthermore, the lowest white arrows in this figure highlight the undesired linear events. As shown in Fig. 13b, following the application of the filter, these events were attenuated and the output data cleaned up. The upper white arrow in parts (a) and (b) highlight the signals at 1300 ms, and the offset at 2800 m; the middle arrow points to the event at 1600 ms, and the offset at 3000 m. At far offsets, these events were masked by refractions and their multiples, a process through which the highlighted events could have been lost, since they go mute as well. Nonetheless, as the equivalent arrows in Fig. 13b shows, by applying the proposed filter, the mentioned events were recovered. Ground roll and aliased ground roll, in this case, were suppressed only in the ground roll fan shaped region (option 1 in step one of the algorithm). The optimum effective parameters are:

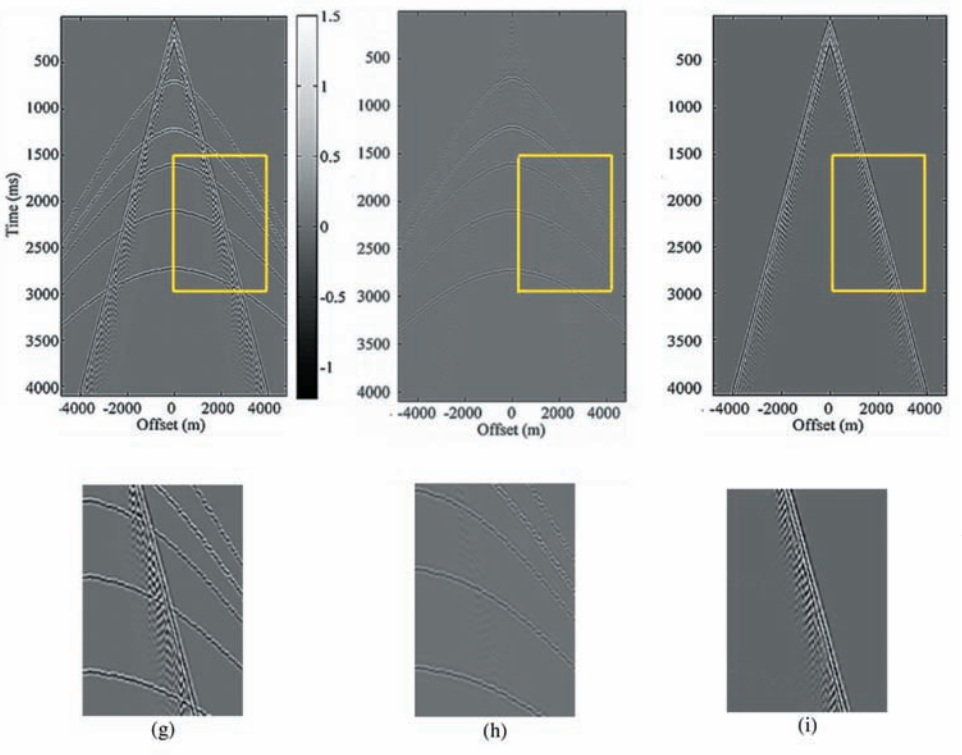

Fig. 8. The effect of random noise and residual statics on ground roll attenuation. (a) Fig. 6a with SNR = 4. (b) After applying the adaptive PDTDFB. (c) The difference between (a) and (b). (d) Fig. 6a with SNR = 2. (e) After applying the adaptive PDTDFB. (f) The difference between (d) and (e). The random noise has no considerable effect on the method. (g) Fig. 6a with residual statics of up to 12 ms. (h) After applying the adaptive PDTDFB. (i) The difference between (g) and (h). To better show the residual static effect in the data, the box part in (g) to (i) are magnified below each part.

- number of levels: 3,
- number of directions: 32,
- range of velocity filter (m/s): 400-1400, and
- number of the selected subscales with higher values of energy: 9.

DISCUSSION

One of the most important parameters in PDTDFB transform is the number of levels and directional subscales in each level of the transform. As illustrated in Fig. 1b, by default, most data energy is concentrated in the center. By increasing the number of the levels, the energy was distributed to other levels and subscales and the size of subscale matrices decreased in each level.

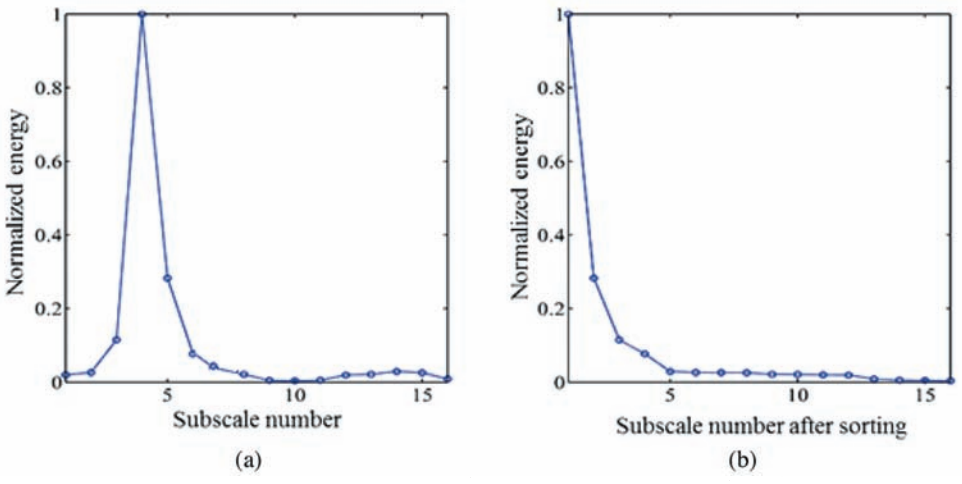

Fig. 9. (a) Normalized energy in the last PDTDFB level of each subscale in the time domain of Fig. 10a. (b) After sorting the normalized energy. Higher values of energy are allocated to subscales containing ground roll and aliased ground roll (for example subscales number 3-7 is part (a) is equal to the first 5 subscales after sorting which contains the ground roll).

It is noteworthy that matrices with very small dimensions are not suitable for use in the proposed algorithm, hence the optimization of the number of levels and subscales. Following a myriad of examinations, three was specified as the optimum number of levels for the synthetic data, the first real data set and the second real data set. In the final level of these data, the numbers of directional decomposed subscales were 16, 16 and 32, respectively. The advantage of PDTDFB over PDFB is that the former uses a dual-tree algorithm ensuing less spatial aliasing problem (because after reconstruction, the aliased data cancel out each other). PDTDFB method, however, produces two sets of decomposed subscales. Furthermore, since PDTDFB is a multi-scale (multi-resolution) method, the events have a similar character in a specific direction in various levels (scales). Accordingly, to save time, the adaptive detection algorithm of the subscales containing ground roll or aliased ground roll was only applied to the final level of one of the two trees. After detecting the subscales primarily containing ground roll or aliased ground roll, they were zeroed in all levels. The filtered data were obtained once the remaining subscales were reconstructed. To better distinguish the subscales containing ground roll or aliased ground roll (according to their energy), a velocity filter was applied to each reconstructed subscale in the time domain after applying the inverse PDTDFB. Selecting a velocity in the velocity range of ground roll is an effective parameter in as far as adaptive PDTDFB performance is concerned.

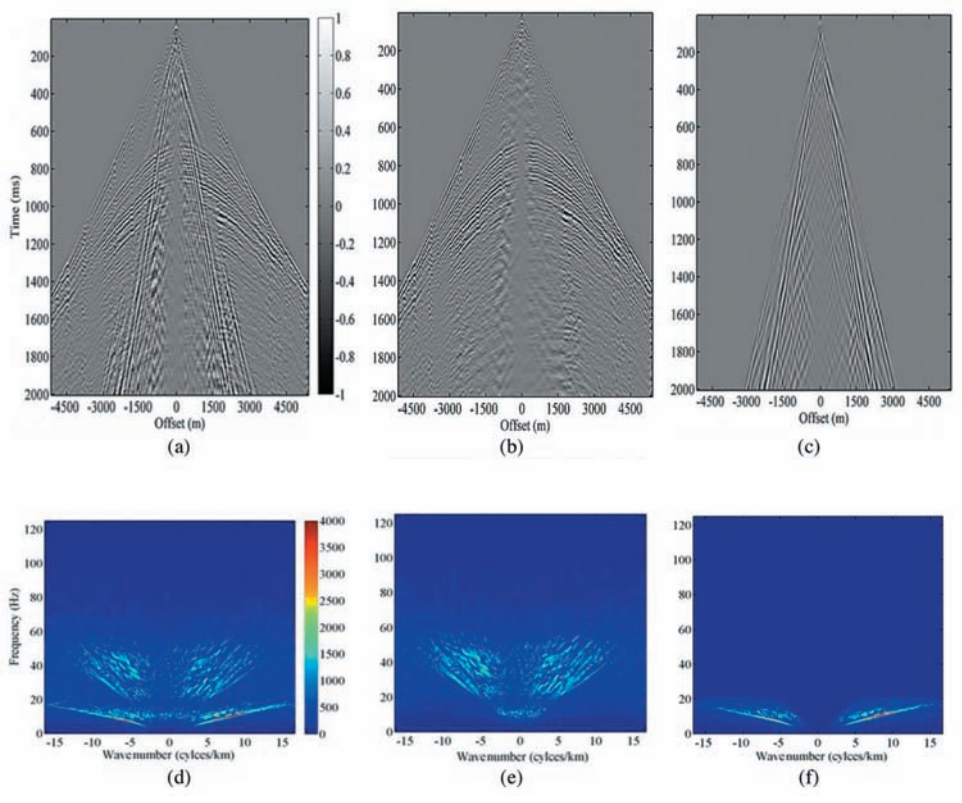

Fig. 10. (a) A real shot record from the west of Iran with a sampling rate of 4 ms and trace spacing of 30 m. (b) After applying the adaptive PDTDFB. (c) The difference between (a) and (b). (d-f) F-k spectra of (a-c).

The most important parameter influencing the performance of adaptive PDTDFB is the number of selected subscales with higher values of energy (as explained in Figs. 5 and 9). As cited in methodology, when subscales with higher energy levels were selected using the sorted energy graph, they were zeroed in all levels while the remaining subscales were reconstructed to achieve the filtered data in step one. Increasing the number of selected subscales, and more ground roll and aliased ground roll are attenuated while more signals may be damaged. On the contrary, by decreasing the number of selected subscales less ground roll and aliased ground roll are attenuated and fewer signals are harmed, hence the fact that the optimum number of subscales has to be specified. In this paper, 4, 5 and 9 were the optimum numbers of subscales for synthetic data, the first real data sets and the second data sets, respectively.

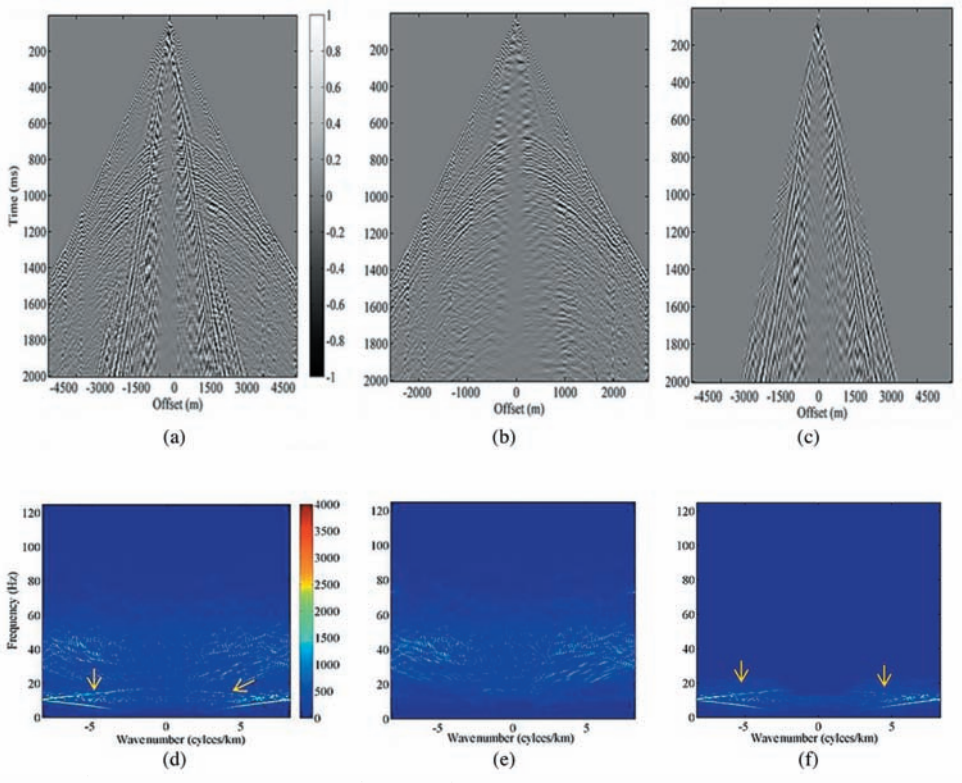

Fig. 11. (a) The real shot record of Fig. 10a after omitting every other trace so as to generate spatial aliasing (b) After applying the adaptive PDTDFB. (c) The difference between (a) and (b). (d-f) F-k spectra of (a-c). The arrows represent the aliased ground roll attenuated in (e).

These values were examined and after conducting many tests the optimum numbers were identified. As mentioned in the methodology, step two was applied in order to attenuate the remaining aliased ground roll in step one. Owing to the similarity of characters between aliased ground roll and back scattered data, the latter data were also attenuated.

As shown in Figs. 6e, 10e and 11e, the results of the adaptive filter in the f-k domain demonstrate that reflections were well preserved, whereas the difference between the input and output of this filter in the f-k domain indicates that ground roll and aliased ground roll were highly attenuated (Figs. 6f, 10f, and 11f). Moreover, the amplitude spectra in Figs. 7 and 12 verify the ability of the adaptive filter to suppress ground roll and aliased ground roll. The arrows

in the f-k spectra of the synthetic data of Fig. 6 and the real data of Fig. 11 demonstrate that the proposed method can substantially attenuate aliased ground roll while properly preserving the reflections. These arrows highlight the advantage of this filter over the f-k filtering method because if f-k filtering were to be employed for attenuating the mentioned aliased ground roll, it would damage the desired signals. In addition, the proposed method uses an adaptive algorithm and discriminates between the subscales containing ground roll or aliased ground roll and those containing reflection events. In f-k filtering, however, the ground roll region must be manually picked, a process which is time-consuming.

Fig. 8 evaluates the performance of the filter in the presence of random noise and residual statics. In Figs. 8a and 8d, different levels of random noise (SNR = 4 and SNR = 2) are examined where the results show that the filter was not too sensitive to the presence of random noise, the reason being that random noise has a very low energy whereas ground rolls are known for their high level of energy. Accordingly, in the sorted energy graph (e.g., Fig. 5b), random noise stands in the last place and cannot affect the subscales containing ground roll. To examine the sensitivity of the filter to the presence of residual statics, residual statics of up to 12 ms were added to the data in Fig. 8g.

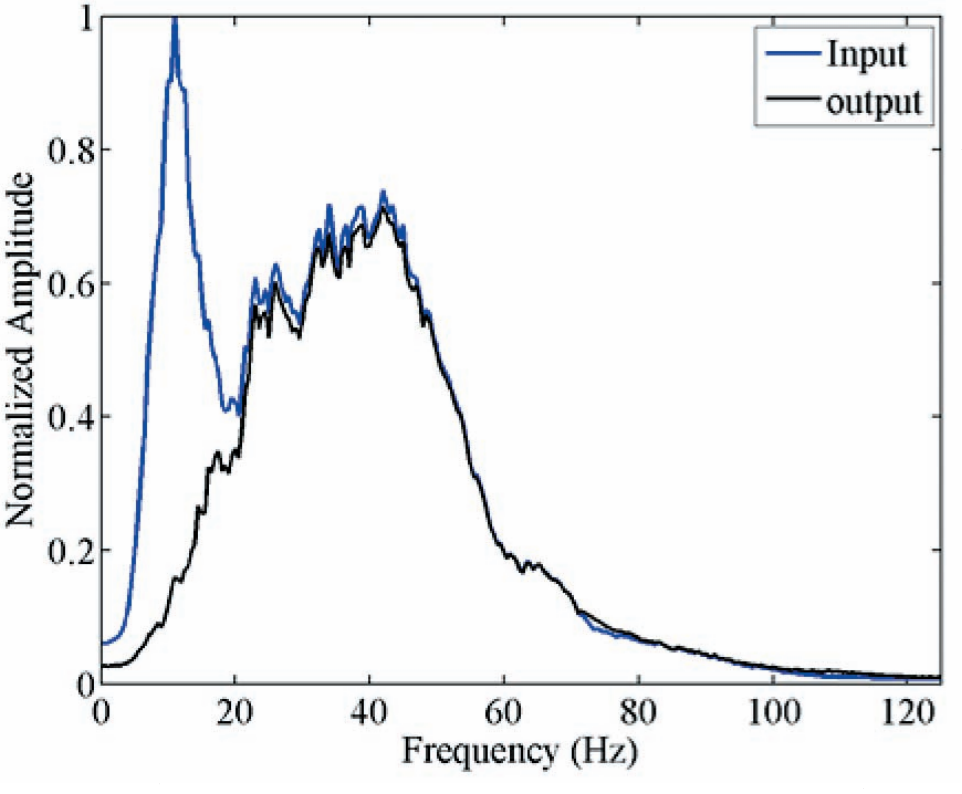

Fig. 12. Amplitude spectra of the input and output related to Fig. 11.

According to the results, except for certain remaining minor residual ground rolls, the filter can attenuate the ground roll in the presence of the residual static problem. Residual statics and the concomitant minor changes in the dip of the ground roll are the reasons behind the presence of the remaining minor ground rolls in the data after applying the filter. These minor changes generate ground roll in the other subscales; therefore minor ground roll remain in the data.

As discussed in the algorithm and effective parameters section, after selecting the first subscales with higher energies in the sorted energy graph (e.g. Fig. 5b), which mainly represent the ground roll and aliased ground roll, there exist two options for applying the adaptive PDTDFB filter. The filter can be applied to the fan shaped ground roll region or all parts of the shot record. Option two (application in the ground roll fan shaped region only) was used for the synthetic data and the first real data sets whereas option one was made use of for the second data set (Fig. 13). Ergo, applying the filter to all parts of the shot record can clean up undesired events outside of the ground roll region and recover the reflection in far offsets from below the refractions. When PDTDFB is applied, events similar to ground roll are placed in the same subscales with ground roll. Therefore after selecting and subsequently zeroing the subscales containing ground roll, the mentioned events are also attenuated.

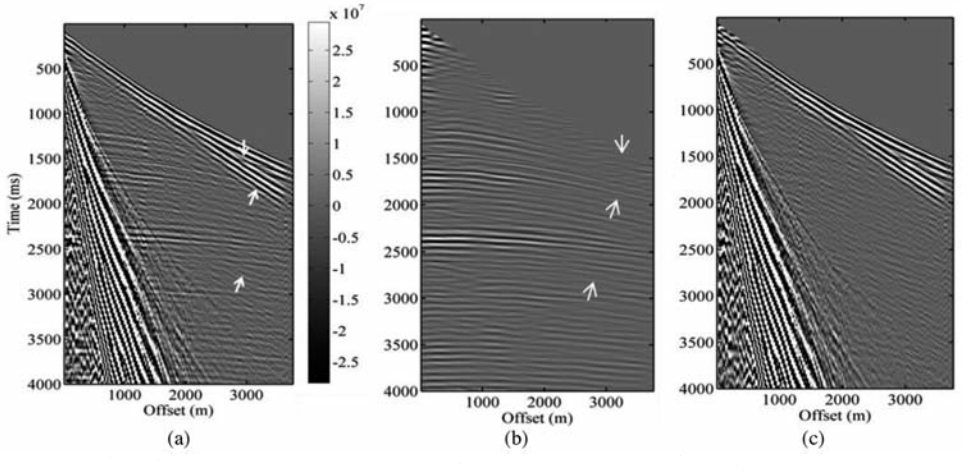

Fig. 13. (a) A real shot record from the south of Iran with a sampling interval of 4 ms and trace spacing of 25 m.(b) After applying the adaptive PDTDFB. (c) The difference between (a) and (b). The two upper white arrows in (a) and (b) show the signal recovering after applying the adaptive PDTDFB and attenuating refractions and their multiples. The lower part of (b) shows the signal enhancement after applying the adaptive PDTDFB and suppressing other undesired events.

To compare the performance of the proposed method with that of a conventional method, the f-k filter was applied to synthetic data in Figs. 6a and 11a using industrial software. Fig. 14a shows the results related to the application of the f-k filter to Fig. 6a with a rejection polygon. In Fig. 14a, the

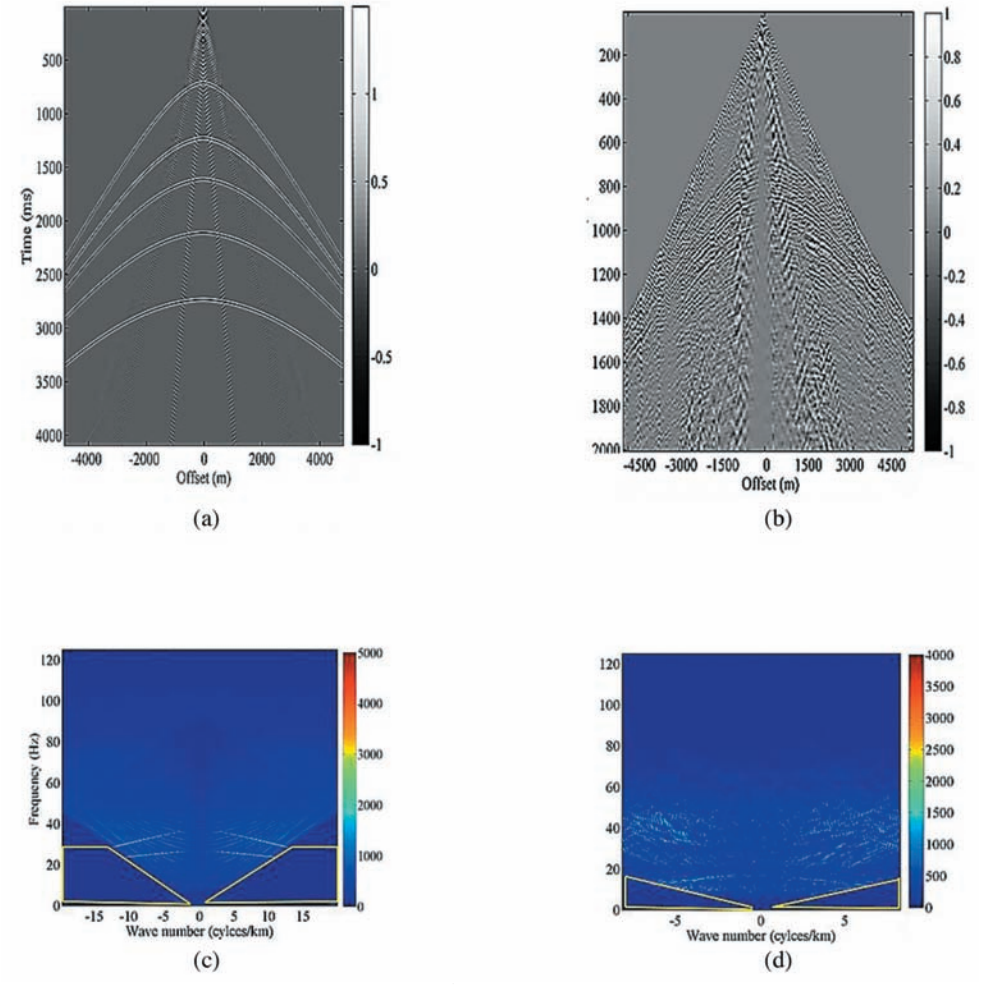

Fig. 14. (a) Fig. 6a after applying f-k filtering using industrial software with rejection polygons in (c). (b) Fig. 11a after applying f-k filtering using industrial software with rejection triangles in (d). (c-d) F-k spectra of (a-b).

rejection polygon was only selected for ground roll attenuation with minimum harm to the signal. It is worth noting that, if all ground roll and aliased groundroll are attenuated, the rejection polygons in the f-k domain will damage the signals. Fig. 14b shows the result of applying f-k filter to the data of Fig. 11a. Parts (c-d) show the f-k spectra of (a-b). The polygons in each figure display the selected rejection polygon. The results show that f-k filtering cannot completely attenuate aliased ground roll without certain damages to the signals. However, according to the results of Figs. 6 and 11, adaptive PDTDFB attenuated the ground roll and aliased ground roll with minimum signal damage. The results qualitatively show that through the use of f-k filtering certain parts of the ground roll and aliased ground roll remain in the data.

To better evaluate and compare the performance of adaptive PDTDFB filter with other common methods, the SVD filter (based on the proposed adaptive singular value decomposition method for ground roll attenuation by Mortazavi and Javaherian (2013)), was applied to the synthetic data. SVD method is an eigen-images decomposition filtering method which, as adduced to in the introduction, can detect and attenuate ground roll in the first eigenimages after flattening. Fig. 15a is the input synthetic data shown in Fig. 6a. Parts (b) and (c) show the results of applying the SVD filter and the difference between the data before and after applying the filter. The results show that SVD filter, unlike the proposed adaptive PDTDFB, cannot attenuate aliased ground roll in a plenary fashion.

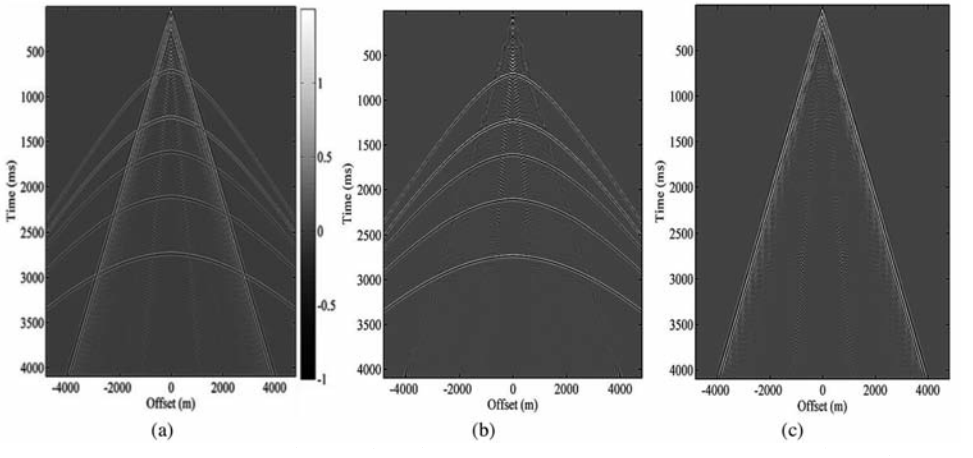

Fig. 15. (a) Input synthetic data (Fig. 6a). (b) Data after applying the SVD filter and (c) the difference between parts (a) and (b).

In order to have a quantitative evaluation of adaptive PDTDFB against the f-k filtering and SVD filtering in ground roll and aliased ground roll attenuation with minimum damage to the signal, a percentage of the attenuated ground roll and aliased ground roll was calculated. Fig. 16a displays the result of synthetic data after applying adaptive PDTDFB; part (b) shows the result of filtered data after applying the f-k filter with the rejection polygon of Fig. 14c and part (c) displays the data after applying the SVD filter. So as to calculate the percentage, the energy of the ground roll and aliased ground roll is calculated in the box of Figs. 16a, (b) and (c). Next, through dividing the calculated energy in the box after applying the filter by the calculated energy of the same box in the input data (for example Fig. 6a), the percentage was specified. The results indicate that adaptive PDTDFB can almost completely attenuate ground roll and aliased ground roll (around 97% ground roll and aliased ground roll attenuation), while via f-k or SVD filtering the ground roll and the aliased ground roll remained in the data. Employing f-k filtering (with a rejection polygon of Fig. 14c), and SVD filtering, 34.2% and 12.3% of ground roll and aliased ground roll, respectively, remained in the data. Moreover, in the SVD method, between the offset range of −1500 to 1500 m and time range of 0 to 2000 ms, more ground roll and aliased ground roll remained in the data. Accordingly, the main advantage of adaptive PDTDFB against f-k and SVD filtering is the aliased ground roll attenuation.

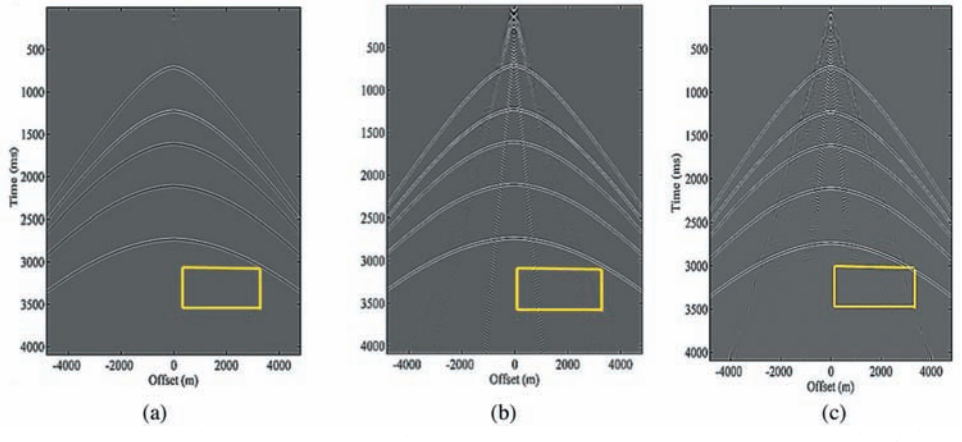

Fig. 16. Synthetic data after applying (a) adaptive PDTDFB. (b) f-k filter and (c) SVD filter. The energy of the remaining ground roll and aliased ground roll is calculated in the box and then compared with the same polygon in input synthetic data (Fig. 6a); the ground roll attenuation percentage is calculated.

CONCLUSIONS

We presented an adaptive ground roll and aliased ground roll attenuation method using adaptive PDTDFB algorithm. By applying this filter to a shot record using a 2-step algorithm, subscales containing ground roll and aliased ground roll were adaptively detected and zeroed, whereby the filtered data was obtained. In the second step, the remaining aliased ground roll was adaptively suppressed. This filter, which can also attenuate refractions and their multiples, was applied to a synthetic shot record containing aliased ground roll and two real shot records from the west and south of Iran. Results showed that this method is able to attenuate ground roll and aliased ground roll with minimum harm to the desired signals, a feature rendering this method superior to f-k filtering. Furthermore, PDTDFB was qualitatively and quantitatively compared with f-k and SVD filtering as two common methods, with the results indicating that the suggested method can attenuate ground roll and aliased ground roll more successfully especially in so far as aliased ground roll attenuation is concerned.

The main effective parameter in this adaptive filter is the selected number of subscales with higher values of energy than others containing the ground roll. The performance of the filter was also examined on a synthetic data set with ground roll in the presence of random noise with SNR = 4, SNR = 2 and residual statics of up to 12 ms. It can be concluded that adaptive PDTDFB is not too sensitive to the presence of random noise and residual statics.

ACKNOWLEDGEMENTS

The authors wish to express their gratitude to NIOC Exploration Directorate, Iran, for the financial support they bestowed upon us and the data they provided through Project No. 89235.The authors also wish to thank Mrs. M. Vefagh for generating the synthetic data.

REFERENCES

Alecu, A., Montesano, A., Pieria, A., Cornelius, J. and Scheele's, P., 2007. On hybrid directional transform-based intra-band image coding. In: Advanced Concepts for Intelligent Vision Systems Lecture Notes in Computer Science. Springer Verlag, Berlin, 4678: 1049-1060.

Bamberger, R.H. and Smith, M.J.T., 1992. A filter bank for the directional decomposition of images: theory and design. IEEE Transact. Signal Process., 40: 882-893.

Bekara, M. and Baan, M.V., 2007. Local singular value decomposition for signal enhancement of seismic data. Geophysics, 72: 59-65.

Boustani, B., Torabi, S., Javaherian, A. and Mortazavi, S.A., 2013. Ground roll attenuation by curvelet-SVD filter: A case study from the West of Iran. J. Geophys. Engineer., 10: 1-10.

Burt, P.J. and Adelson, E.H., 1983. The Laplacian pyramid as a compact image code. IEEE Transact. Communic., 31: 532-540.

Chang, G.L., Hong, X.C., Ye, L.J., Jing, D. and Wen, J.S., 2011. Seismic noise attenuation using nonstationary polynomial fitting. Appl. Geophys., 8: 18-26.

Do, M.N. and Vetterli, M., 2001. Pyramidal directional filter bank and curvelets. IEEE Internat. Conf. Image Process. (ICIP), Thessaloniki, Greece.

Do, M.N. and Vetterli, M., 2005. The contourlet transform: An efficient directional multiresolution image representation. IEEE Transact. Image Process., 14: 2091-2106.

Hamidi, R., Javaherian, A. and Reza, A.M., 2013. Comparison of 1DWT and 2DWT transforms in ground roll attenuation. J. Seismic Explor., 22: 49-76.

Henley, D.C., 1999. Coherent noise attenuation in radial trace domain: introduction and demonstration. CREWES Res. Rep., 11.

Henley, D.C., 2003. Coherent noise attenuation in the radial trace domain. Geophysics, 68: 1408-1416.

Herrmann, R.B., 2013. Computer programs in seismology. An evolving tool for instruction and research. Seism. Res. Lett., 84: 1081-1088.

Hosseini, S.A., Javaherian, A., Hassani, H., Torabi, S. and Sadri, M., 2015. Shearlet transform in aliased ground roll attenuation and its comparison with f-k filtering and curvelet transform. J. Geophys. Engineer., 12: 351-364.

Khan, M.A.U., Khalid Khan, M. and Aurangzeb Khan, M., 2004. Coronary angiogram image enhancement using decimation-free directional filter banks. Internat. Conf. Acoust., Speech, Sign. Process.: 441-444.

Liu, X., 1999. Ground roll suppression using the Karhunen-Loeve transform. Geophysics, 64: 564-566.

Lu, W., 2006. Adaptive noise attenuation of seismic images based on singular value decomposition and texture direction detection. J. Geophys. Engineer., 3: 28-34.

Ma, S.F., Zheng, G.F., Jin, L.X., Han, S.L. and Zhang, R.F., 2010. Directional multiscale edge detection using contourlet transform. 2nd Internat. Conf. Adv. Comput. Contr., Shenyang: 58-62.

Manentti, R. and Porsani, M.J., 2013. Ground roll attenuation applying adaptive singular value decomposition method in the radial domain. Expanded Abstr., 83rd Ann. Internat. SEG Mtg., Houston: 4402-4406.

Mortazavi, S.A. and Javaherian, A., 2013. The effect of signal-to-noise ratio on ground roll attenuation using adaptive singular value decomposition; A case study from South West of Iran. J. Seismic Explor., 22: 427-447.

Nguyen, T., 2006. The Multiresolutional Directional Filter Bank. Ph.D. thesis, The Univ. of Texas, Arlington, TX.

Niu, P., Wang, X. and Lu, M., 2011. A novel pyramidal dual-tree directional filter bank domain color image watermarking algorithm ICICS'11. Proc. 13th Internat. Conf. Informat. Communicat. Secur.: 158-172. Springer-Verlag, Berlin.

Porsani, M.J., Silva, M.G., Melo, P.E.M. and Ursin, B., 2010. SVD filtering applied to ground roll attenuation. J. Geophys. Engineer., 7: 284-289.

Tyapkin, Y.K., Marmalyevsky, N.Y. and Gornyak, Z.V., 2003. Source generated noise attenuation using the singular value decomposition. Expanded Abstr, 75th Ann. Internat. SEG Mtg., Houston: 2044- 2047.

Yarham, C., Boeniger, U. and Herrmann, F.J., 2006. Curvelet-based ground roll removal. Expanded Abstr., 78th Ann. Internat. SEG Mtg., New Orleans: 2777-2782.

Yilmaz, O., 2001. Seismic data analysis: processing, inversion and interpretation of seismic data (Vols. 1 & 2). SEG, Tulsa, OK.

Zhang, Z.Y., Zhang, X.D., Yu, H.Y. and Pan, X.H., 2010. Noise suppression based on a fast discrete curvelet transform. J. Geophys. Engineer., 7: 105-112.